REPORT DOCUMENTATION PAGE

Form Approved
OMB No 0704-0188

Public reporting burden for this collection of information is estimated to average 1 hour per response, including the time for reviewing instructions, searching existing data sources, gathering and maintaining the data needed, and completing and reviewing the collection of information. Send comments regarding this burden estimate or any other aspect of this collection of information, including suggestions for reducing this burden, to Washington Headquarters Services, Directorate for Information Operations and Reports, 1215 Jefferson Davis Highway, Suite 1204, Arlington, VA 22202-4302, and to the Office of Management and Budget, Paperwork Reduction Project (0704-0188), Washington, DC 20503

1. AGENCY USE ONLY (Leave blank)	2. REPORT DATE	3. REPORT TYPE AND DATES COVERED
		FINAL

4. TITLE AND SUBTITLE
Thin Film Routes to New Materials

5. FUNDING NUMBERS

61102F

2305/GS

6. AUTHOR(S)
Prof Arthur W. Sleight

7. PERFORMING ORGANIZATION NAME(S) AND ADDRESS(ES)
Dept of Chemistry
Oregon State Univ
Corvallis, Oregon 97331-4033

8. PERFORMING ORGANIZATION REPORT NUMBER

AFOSR-TR 95-0307

9. SPONSORING MONITORING AGENCY NAME(S) AND ADDRESS(ES)
AFOSR/NE
110 Duncan Avenue Suite B115
Bolling AFB DC 20332-0001

10. SPONSORING MONITORING AGENCY REPORT NUMBER

F49620-92-J-0028

11. SUPPLEMENTARY NOTES

12a. DISTRIBUTION AVAILABILITY STATEMENT

APPROVED FOR PUBLIC RELEASE: DISTRIBUTION UNLIMITED

12b. DISTRIBUTION CODE

DTIC
ELECTE
JUN 21 1995
F

13. ABSTRACT (Maximum 200 words)

SEE FINAL REPORT ABSTRACT

DTIC QUALITY INSPECTED 5

14. SUBJECT TERMS			15. NUMBER OF PAGES
			16. PRICE CODE

17. SECURITY CLASSIFICATION OF REPORT	18. SECURITY CLASSIFICATION OF THIS PAGE	19. SECURITY CLASSIFICATION OF ABSTRACT	20. LIMITATION OF ABSTRACT
UNCLASSIFIED	UNCLASSIFIED	UNCLASSIFIED	UNCLASSIFIED

Final

~~SECOND ANNUAL~~ TECHNICAL REPORT

NOVEMBER 1, 1993 - OCTOBER 31, 1994

Contract F49620-92-J-0028

Air Force Office of Scientific Research

Thin Film Routes to New Materials

Arthur W. Sleight

Department of Chemistry

Oregon State University

Corvallis, Oregon 97331-4033

19950616 077

Summary

Most of the effort for the three years of this project was spent on the synthesis and characterization of cuprates with the infinite layer structure. For that reason, a detailed description of that work is included in this report. Our effort using LiF as a substrate was introduced in our last report. This work has continued and has lead to the deposition of Cu_4O_3 films on LiF. This is a form of copper oxide known as mineral, but it has apparently never before been synthesized by man.

Reported critical currents for $YBa_2Cu_3O_7$ are higher in thin films than in single crystals. It appears that this is related to a higher concentration of Y/Ba antisite disorder in thin films. Such antisite disorder is expected to increase as the size of the rare earth increases. Thus, we grew single crystals of $NdBa_2Cu_3O_7$ to see if such crystals would show higher critical current than $YBa_2Cu_3O_7$ crystals. We found, however, that the synthesis procedure that results in high quality $YBa_2Cu_3O_7$ crystals of does not yield high quality crystals of $NdBa_2Cu_3O_7$.

Thin Films of Cuprates with the Infinite Layer Structure
Summary

Thin films of $Sr_{1-x}CuO_{2-\delta}$ with the infinite-layer structure were prepared using the single target rf-magnetron sputtering method. The substrate was MgO or $SrTiO_3$ in an off-axis configuration. Previous reports have focused on films prepared on MgO substrates. This report focuses on films prepared on $SrTiO_3$ substrates. The structure and the electrical properties of the films were found to be sensitive to the oxygen pressure during sputtering. Quantitative analysis of X-ray diffraction data indicated that films formed under lower oxygen pressure possessed a larger concentration of defects and higher electrical resistivities. The highest conductivity was observed in a film which contained two infinite-layer phases, one with a relatively low concentration of defects and another with a higher concentration of defects. A discussion is given of the necessary corrections that must be made in order to quantitatively evaluate epitaxial thin film X-ray diffraction intensities measured with a $\theta-2\theta$ diffractometer.

Introduction

The so called infinite-layer(IL) structure, a tetragonal phase with an ideal composition of $SrCuO_2$, has the simplest structure containing the CuO_2 planes which are considered essential for the occurrence of high temperature superconductivity[1]. Using normal synthesis procedures in air, only compositions of the type $Sr_{1-x}Ca_xCuO_2$ with x close to 0.85 can be prepared. Under high pressure or by epitaxial growth of thin films on a substrate, the IL-structure can be chemically doped to be superconducting. For example, partial substitution of a large rare-earths such as La, Sm, Nd or Gd for Sr[2-4] can yield electron-doped superconductors with transition temperatures(T_c) of about 40 K. Superconductors of the IL-phase with higher T_cs of about 60-110 K were reportedly formed by partial substitution of Ca or Ba for Sr under high pressure[5-7]. These superconductors may be hole-doped by introducing vacancies into the alkaline-metal lattice sites. Although the superconductivity is well established in Ba/Sr/Ca/Cu/O samples prepared at high pressure, the composition and precise structure of the superconducting phases are unclear. Hiroi et al.[7] observed planar defects parallel to the CuO_2 planes in alkali-metal deficient superconductors and suggested that these defect layers may act as a "charge reservoir" and be the key factor for presence of superconductivity. Adachi et al. have argued that their is no compelling evidence for superconductivity in p-doped IL phases prepared at high pressure[8].

Attempts to prepare of hole-doped superconducting IL samples using epitaxial thin film growth methods have not yet been successful[9-12]. Despite the lack of superconductivity, these studies provide some interesting information about the structure and physical properties of IL films. N. Sugii et al.[10] observed the intergrowth of Sr_2CuO_3 and IL $SrCuO_{2-\delta}$, and they

suggested that superconductivity could not exist without Sr-deficient defect layers. R. Feenstra et al.[11] suggested that electron-doped $Sr_{1-x}CuO_{2-\delta}$ films are associated with Sr point defects of an undefined nature, while intergrowth with SrO_{1-x} defect layers may lead to hole-doping. Yakabe et al.[12] suggested that the reason for the absence superconductivity in hole-doped IL-thin films can be attributed to an insufficient number of charge carriers in the CuO_2 planes or to structural rearrangement associated with the defects. The debate in the literature indicates that further studies are necessary to better understand the structure and physical properties of IL compounds, as well as to continue the search for new superconducting phases with the parent IL $ACuO_2$ structure. Our films were grown under different conditions than those used in previous studies, apparently leading to IL films with structures and properties different from those previously reported.

We report here the results of the synthesis and characterization of a series of $Sr_{1-x}CuO_{2-\delta}$ IL-thin films. Compared to previous studies on similar compositions[9-11], we prepared IL phases under higher oxygen pressure and focused our study on how synthesis conditions such as oxygen pressure affect the structure and the electrical properties of the films. We found that the electrical properties of the films are very sensitive to the oxygen pressure during the film growth. The IL-structures obtained are not very stable, especially those films prepared under our highest oxygen pressures. Quantitative structure analyses indicate that IL structures with a high concentration of defects and relatively high electrical resistivity are formed under low oxygen pressure, while films of lower electrical resistivity are formed in higher oxygen pressure. The relationships between the structure and the electrical properties of these films are discussed in conjunction with the quantitative structural analysis and post-annealing results.

Experimental

$Sr_{1-x}CuO_{2-\delta}$ thin films were grown in an off-axis single target rf-magnetron sputtering system. Two kinds of ceramic targets of nominal composition of $Sr_{1-x}CuO_{2-\delta}$ and $Sr_{1-x}Pb_xCuO_{2-\delta}(x=0.1, 0.5)$ were prepared by high temperature solid state reaction.using $SrCO_3$, CuO, and PbO. Despite the presence of lead in the some targets (the lead was initially present in order to attempt deposition of n-doped IL films), subsequent electron microprobe chemical analysis showed no traces of lead in the films. A $SrTiO_3$(STO) single crystal wafer cut in a 001 orientation was used as the substrate. The substrate temperature was kept at 600 °C during the deposition. The target to substrate distance was about 8 cm. During the deposition, the Ar gas pressure was about 20 mTorr. The oxygen pressure was varied from 1 mTorr to 40 mTorr in different deposition runs. It was found that low oxygen pressure(< 5 m Torr) led to multiple phase thin films. After deposition, an oxygen pressure of a few Torr was quickly established in

the chamber, and the film was cooled quickly to room temperature. The films thicknesses were about 2000 Å as measured using the Stylus method. X-ray diffraction patterns of the films were obtained with a Siemens D-5000 powder diffractometer using Cu K_α radiation. Data were collected over the 2θ range of 2°-150° using a step size of 0.01° and counting for 2s at each step. The electrical resistivities of the films were measured by the standard four-probe AC method in the temperature range of about 300 K to 4.2 K. Typically the current applied was about 0.1 mA. For some measurements, a very small current of 0.01 µA was applied in order to check anomalous behavior of temperature-dependent resistivity at low temperatures.

Results

Structural Studies

As described previously, 20 mTorr Ar gas and 1mTorr to 40 mTorr oxygen gas were used during the film deposition. We found that film structure and quality was sensitive to the oxygen pressure. Low oxygen pressure during deposition (< 5mTorr) led to multiple phase films. High oxygen pressure during deposition (> 30mTorr) gave unstable films which will be discussed in more detail later. All the $Sr_{1-x}CuO_{2-\delta}$ films grown in an oxygen pressure of 5 mTorr to 25 mTorr appear to be single phase and have the IL structure. These films grow epitaxially with the c-axis parallel to the substrate. Fig. 1(a) shows a typical X-ray diffraction pattern of a film. All of the significant peaks in the pattern are either the (00ℓ) peaks of IL-phase or can be attributed to the STO substrate. A rocking curve analysis of the (001) peak gives a FWHM of about 0.2° (Fig. 1 (b)) indicating good epitaxy and a fairly high degree of crystallinity. The c-lattice parameters of the films obtained in different oxygen gas pressures are different, even for the films using the same target. It is found that the lower the oxygen pressure the larger the c-axis lattice parameter.

Besides c-lattice parameters, the intensity ratios of (00ℓ) peaks are also very different for films grown under different oxygen pressure. In fig. 2 we show several X-ray diffraction patterns of films with the IL-structure. For clarity, the intensity of each pattern was normalized to the 002 reflection, and the horizontal axes (2θ) of each pattern were shifted about 2° relative to each other. The intensity of 004 reflection is low, so the 004 peaks in fig. 2 were enlarged by factor of ten. In fig. 2, it is apparent that the intensity ratio of the 001 peak to the 002 peak decreases with increasing oxygen pressure. In addition, one can find that the peak shape of film 4 grown in 25 mTorr is quite different from that of the other films. Further peak profile analysis indicates that there are actually two phases in film 4 (figure 3).

The X-ray diffraction intensities of the (00ℓ) peaks are very sensitive to the sample mounting position. In order to obtain accurate peak intensities, the most intense peak (002) was maximized in intensity by comparing the angle deviation, $\Delta\theta$, between the theta value obtained
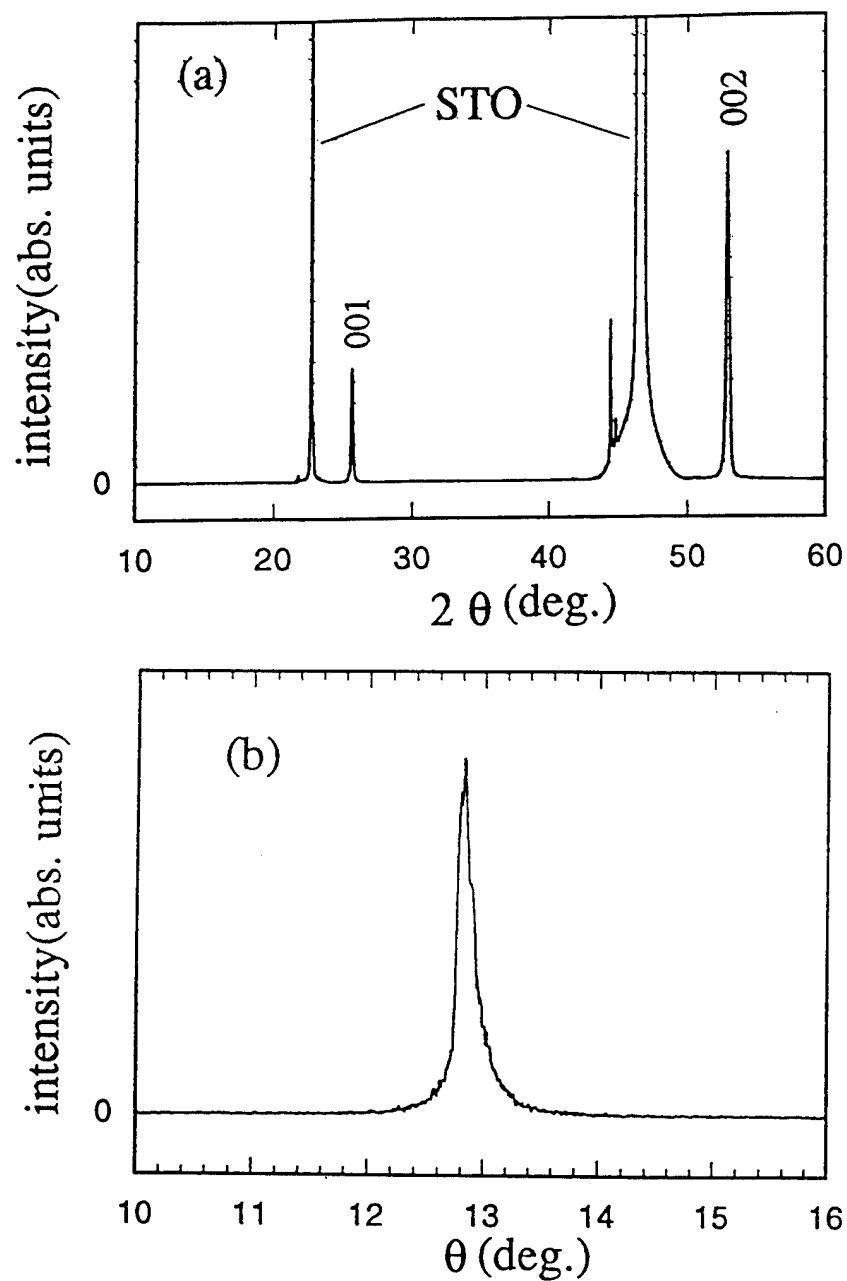
Fig. 1 (a) X-ray diffraction pattern of a typical as-grown film. All peaks can be attributed to 00ℓ IL reflections or to the SrTiO$_3$ substrate. (b) (00ℓ) of rocking curve of the IL phase gives a FWHM of about 0.2° indicating good epitaxy and a high degree of crystallinity.
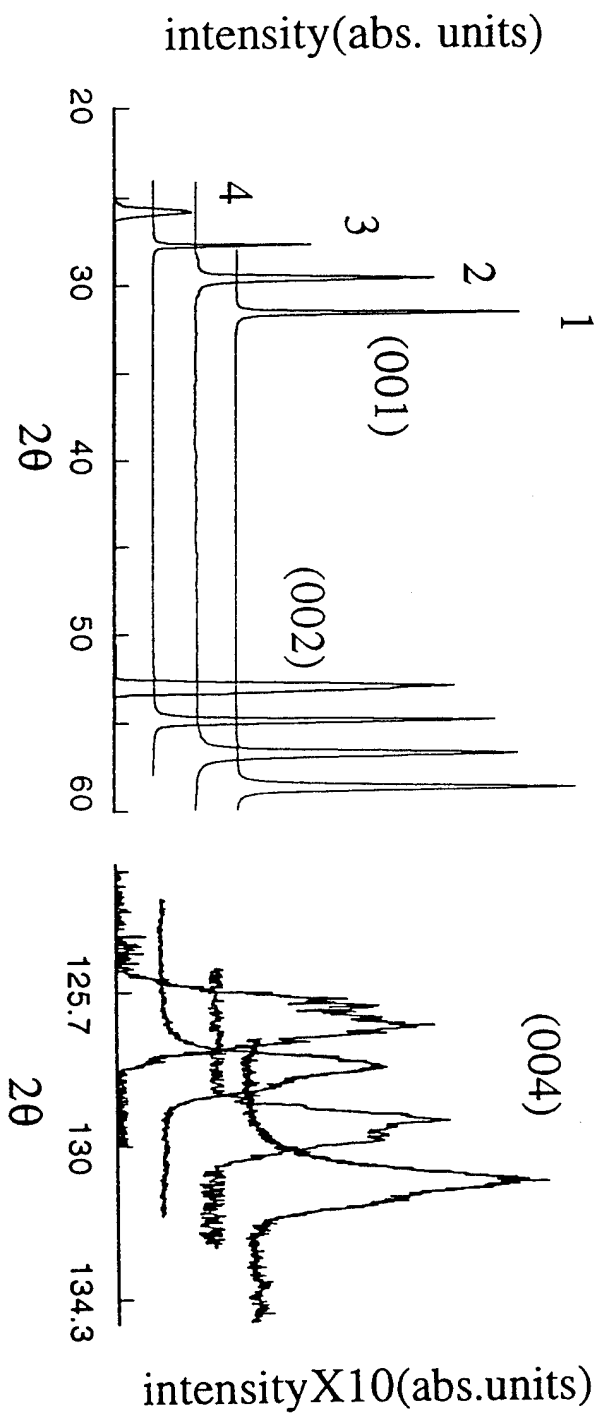
Fig. 2 X-ray diffraction patterns of films grown under different oxygen pressures. For film 1 to 4, the oxygen pressures used are 5 mTorr, 7.5 mTorr, 10 mTorr and 25 mTorr, respectively. The intensities of all peaks are normalized to the (002) peak. For a better illustration, the intensity scale of the (004) peaks is enlarged by a factor of 10.

Fig. 3 Profile fitting of the (004) reflection peak of film 4 assuming two phases to be present. The thin solid line is the observed peak profile. The thick solid line is the fitting profile. The dashed and dotted lines are $K_{\alpha 1}$ and $K_{\alpha 2}$ reflections of phase 1 and 2, respectively.

from the peak position of a rocking curve analysis, θ_{rc}, and one half of the 2θ value obtained in a normal θ-2θ scan, θ_n ($\Delta\theta = |\theta_{rc}-\theta_n|$). If the value of $\Delta\theta$ was greater than 0.02°, the film was remounted. Moreover, the divergence and antiscatter slits on the diffractometer were computer controlled so that the irradiated area was maintained constant, independent of theta. The irradiated area was larger than the sample so that the entire thin film was irradiated throughout the measurement. As will be discussed in more detail later, the films were thin enough so that the x-rays were not significantly attenuated even at the bottom of the films. These two considerations taken together insure that the entire sample volume was irradiated throughout the entire θ-2θ scan. In powder diffraction of thick samples, the irradiated area decreases and the penetration depth increases as theta increases. As long as nearly all of the X-rays are attenuated by the sample (infinitely thick limit), these two effects effectively cancel each other and result in an irradiated volume that is constant with changing theta. Here we are in the infinitely thin limit, and through the use of computer controlled slits the irradiated volume can be maintained constant throughout the scan. However, the X-ray flux on the sample increases with increasing theta in a known fashion. The deviations of the intensity ratios of (00ℓ) peaks in different measurements of the same film were less than 5% when $\Delta\theta < 0.02°$.

If the proper precautions have been taken to insure that accurate peak intensities are obtained, one can extract information regarding the not only the dimensions but the contents of the unit cell. In the measurement of a polycrystalline sample, the relative intensity of an *hkl* reflection is given by the expression:

$$I = S\,|F|^2\,M\,L_p\,A\,E\,B_t + B_g,$$

where I is the intensity of the reflection, S is a scale factor, F is the crystal structure factor, M is the multiplicity, L_p is the Lorentz-Polarization factor, A is an absorption correction, E is an extinction correction, B_t is an overall temperature factor, and B_g is a term representing the background contribution to the intensity. All of the structural information is contained in the F term, but the other corrections must be properly calculated in order to extract accurate structural information from peak intensities. When considering a perfectly epitaxial thin film sample, some of these terms are somewhat different than in ordinary powder diffraction. The scale factor S is simply a scaling term and is the same for all reflections in the pattern. In this analysis the scale factor has been chosen so that the (002) peak always has an intensity of 1000. The multiplicity, M, is always 2 for (00ℓ) reflections in a tetragonal space group.

Primary extinction is likely to be a serious problem in epitaxial films if they are thick enough. However the films prepared in this study, have thicknesses less than 0.5 microns and generally on the order of 0.2 microns and are therefore, very thin compared to normal perfect crystals. Taking this into consideration, the extinction correction can be neglected.

In the earlier discussion, it was stated that diffraction from these films fell into the infinitely thin limit; therefore, no correction for absorption is required. In order to more rigorously prove this and also as a consideration for analyses of other thin film samples, the proper absorption correction for this experimental configuration will be derived. For diffraction from a (00ℓ) plane, the intensity of radiation scattered from a layer of length ℓ, width w (into the plane of the paper of Fig. 4), and thickness dz, located at a depth z below the surface is (see fig. 4):

$$dI_d = \alpha I_o e^{-\mu D} dV$$

where α is the fraction of incident energy diffracted per unit volume of the crystal, D is the path length of the X-ray beam throught the sample, and μ is the linear absorption coefficient of the material. Considering the geometry of a Bragg reflection shown in fig. 4, the above expression can be rewritten to be:

$$dI_d = \alpha I_o e^{-\mu(AB+BC)} (\ell w dz),$$
$$dI_d = (\alpha I_o)e^{-\mu(2z/\sin\theta)} dz,$$

In a typical fixed slit geometry, the irradiated width w is constant and the irradiated length ℓ is proportional to $1/\sin\theta$. However when computer controlled variable slits are used as they were in this study, both ℓ and w are constant, so that integrating dI_d from 0 to T, where T is the thickness of the film gives:

$$I_d = (\alpha lwI_o/2\mu) \sin\theta (1-e^{-\mu 2T/\sin\theta}).$$

The first term is just a constant which is independent of two-theta and can be incorporated into the scale factor. The second and third terms describe the theta dependence of the absorption correction to the reflection intensities. Fig. 5 shows this plot for different film thicknesses using a linear absorption coefficient of 370 cm^{-1} (calculated based on the density of $SrCuO_2$). For film thicknesses less than 0.5 microns (5000 Å) and peaks with two-theta values greater than 15-20° the absorption correction is negligible and can be ignored.

The standard Lorentz-Polarization correction for powders is:

$$L_p = (\text{Lorentz Factor})(\text{Polarization}) = (1/(\sin 2\theta \sin\theta))((1+\cos^2 2\theta)/2),$$
$$L_p = (1+\cos^2 2\theta)/(2\sin 2\theta \sin\theta) \ [13].$$

However, an epitaxial thin film does not have a random orientation of grains like a powder sample is assumed to have, and can be treated as a single crystal rather than a powder. This does not affect the polarization term but does effect the Lorentz correction. The Lorentz factor for single crystal reflections from planes parallel to the ϕ axis was first derived by Darwin[14] and is appropriate for epitaxial thin films in the Bragg-Bretanno geometry. Combining this with the polarization term gives:

$$L_p = (2/\sin 2\theta)((1+\cos^2 2\theta)/2),$$
$$L_p = (1+\cos^2 2\theta)/(\sin 2\theta).$$

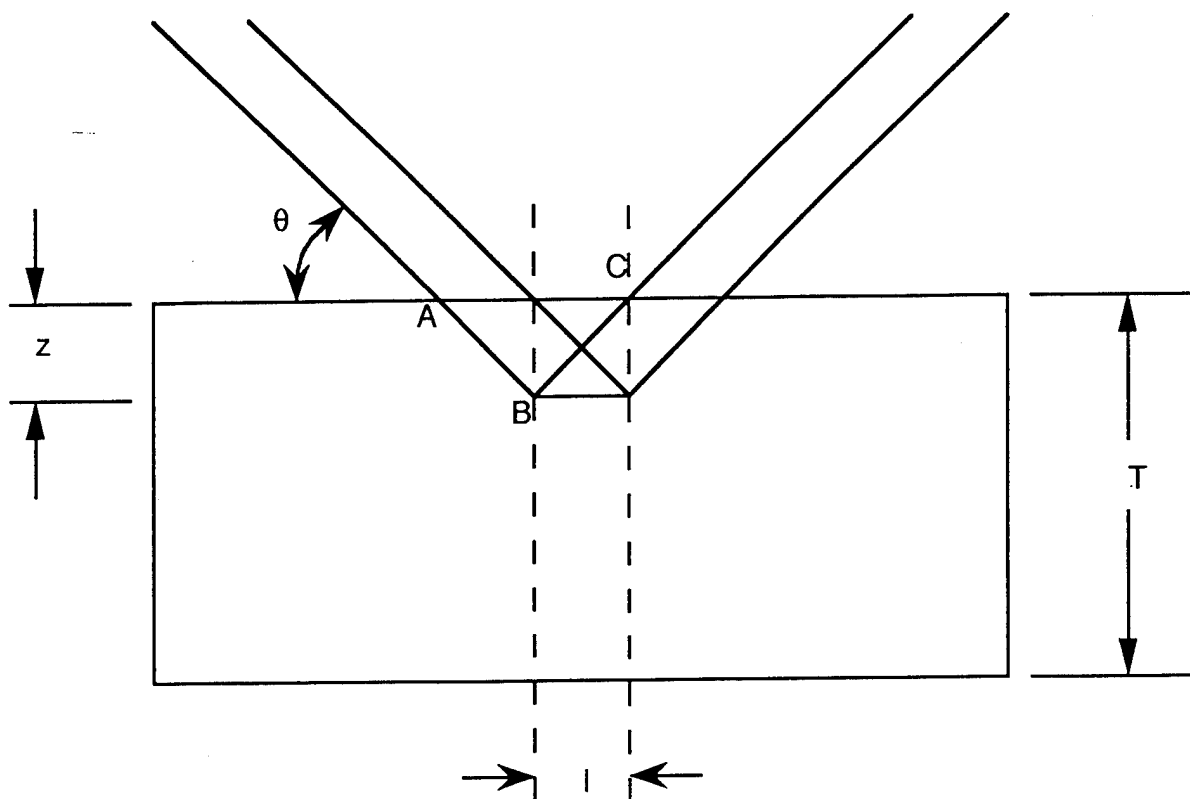Note that this expression is different from the standard L_p correction by $1/\sin\theta$.

Fig. 4 Schematic representation of the geometry associated with diffraction of X-rays from a (001) plane of an epitaxial thin film in the Bragg-Bretanno geometry.
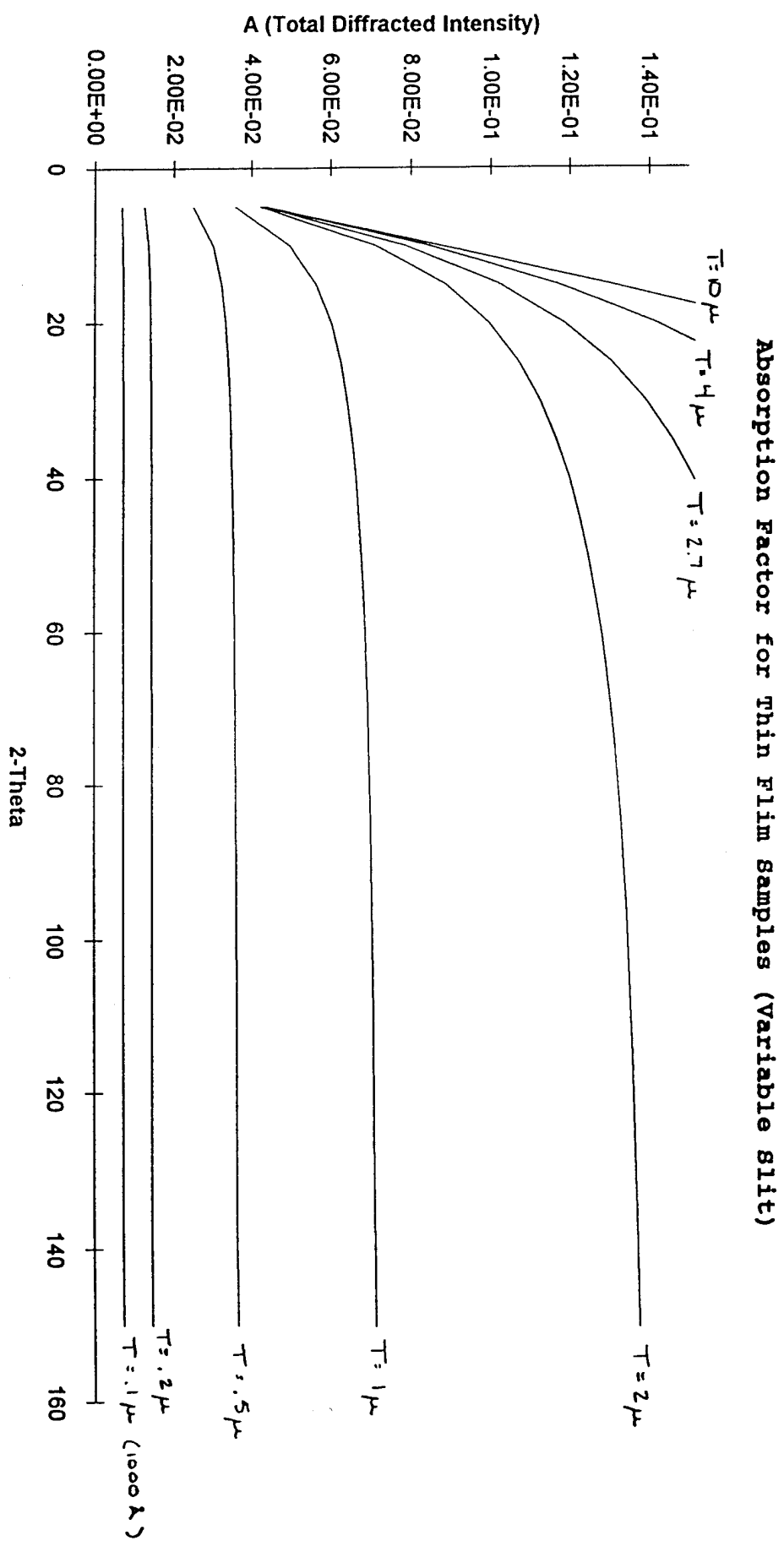
Absorption Factor for Thin Film Samples (Variable Slit)

A (Total Diffracted Intensity)

T = 0 μ   T = .4 μ   T = 2.7 μ

T = 2 μ

T = 1 μ

T = .5 μ

T = .2 μ
T = .1 μ (1000 Å)

2-Theta

Fig. 5 The theta dependence of absorption correction to the reflection intensities for different
film thicknesses.

The correction for thermal motions of the atoms is usually applied to the scattering factor of each atom individually. However, in order to minimize correlation with occupancies, an overall thermal parameter was used to account for thermal motions of the atoms. The standard expression used to account for harmonic thermal motion of the atoms is [13]:

$$B_t = \exp[-2B(\sin\theta/\lambda)^2],$$

where B is the overall thermal parameter and λ is the wavelength of radiation used.

Two groups have recently reported the quantitative structural analysis of c-axis oriented $YBa_2Cu_3O_7$ thin films[15,16]. Quantitative structural information such as antisite disorder between Y and Ba cations and the oxygen content in the films were obtained. Such refinement results should be reliable when the fitting parameters or variables are limited and the proper corrections have been made to the intensities, as discussed above. Compared to $YBa_2Cu_3O_7$, the infinite-layer crystal structure is simpler. Thus, even though there are fewer (00ℓ) reflections, a similar refinement technique can be applied to the analysis of IL structures. The usual tetragonal IL structure in space group P4/mmm (#123) was assumed. In table 1 we list the crystallographic data used for the structure refinement. The intensities of (001), (002), (003) and (004) peaks were used for the refinements.

Table 1. Crystallographic data of infinite-layer structure $SrCuO_2$.
Space group: P4/mmm (no. 123)

atom	position	x	y	z
Sr	1d	1/2	1/2	1/2
Cu	1a	0	0	0
O	2f	0	1/2	0

As can be seen in Fig. 2, the intensity ratios of the 001 to the 002 peak are significantly in different films. Calculation of the structure factor for (00ℓ) reflections gives the expression:

$$F(00\ell) = F(x,y,0) + F(x,y,1/2)\cos\pi\ell,$$

where F(x,y,0) represents the sum of the atomic scattering factors of all of the atoms located in the plane with z = 0, and F(x,y,1/2) is the sum of the atomic scattering factors of all atoms located in the z = 1/2 plane. This shows that when ℓ is even the structure factor will be the sum of all of the atomic scattering factors in the structure and when ℓ is odd it will be the difference between the electron density in the z = 0 layer and the z = 1/2 layer. Therefore, it is possible to adjust the overall B value to obtain the proper intensity ratio between, for example, the (002) and (004) reflections because this ratio is only very weakly dependent upon the occupancies of the different crystallographic sites. Once that has been done, the defect concentration can be adjusted to give the proper ratio between the (001) and (002) reflections. The very weak (003)

reflection can then be used as a check on the accuracy of the defect concentration and overall thermal parameter. In this way, solutions can be obtained by calculating the structure factors for different defect concentrations and models with the program LAZY/PULVERIX and applying the proper corrections to it. This is done in table 2, where the structural model used in the LAZY/PULVERIX program is $Sr_{1-x}CuO_{2-x}$. The rationale for using the charge compensated defect model in the structure factor calculation is discussed in more detail later. The defect concentration, c lattice parameter, zero point, and overall thermal parameter for each film are given in table 3. Note the zero point corrections are all quite small and consistent with the zero point corrections normally found for well mounted powder samples in our instrument. This is an indication that minimizing $\Delta\theta$ results in samples that are correctly mounted with the proper height and orientation. It is also further evidence that the reflection intensities obtained in this study are reliable.

Table 2. Structure factors calculated with the program of LAZY/PULVERIX

film	P_{O_2}(m Torr)	h k l	intensity(obsv.)	LP	Mult.	Temp. factor	F^2	intensity(cal.)
1	5	001	890	2.1	2	0.87	242	884
		002	1000	0.86	2	0.57	1023	1003
		003	5	0.51	2	0.28	42	12
		004	59	0.81	2	0.10	345	56
3	10	001	454	2.09	2	0.85	128	455
		002	1000	0.86	2	0.53	1100	1002
		003	2	0.51	2	0.24	15	4
		004	50	0.83	2	0.08	381	51
4	25	001	238	2.09	2	0.86	67	240
phase 1		002	1000	0.86	2	0.53	1093	1000
		004	52	0.81	2	0.08	387	52
phase 2		001	584	2.08	2	0.86	168	599
		002	1000	0.85	2	0.55	1071	1000
		004	57	0.85	2	0.09	369	57

Electrical properties

All films showed semiconducting behavior. The resistivity of the films depend strongly on the oxygen pressure during the deposition (table 3). When the oxygen pressure increased from 5 mTorr to 25 m Torr, the resistivity of the film decreased from 24 Ω-cm to 0.04 Ω-cm. It is interesting to note that a highly-defect IL structure does not necessarily produce a film with low electrical resistivity. Besides the magnitude of the resistivity, the temperature dependence of the resistiviy varies for the different films (Fig. 6). This behavior is not consistent with thermal
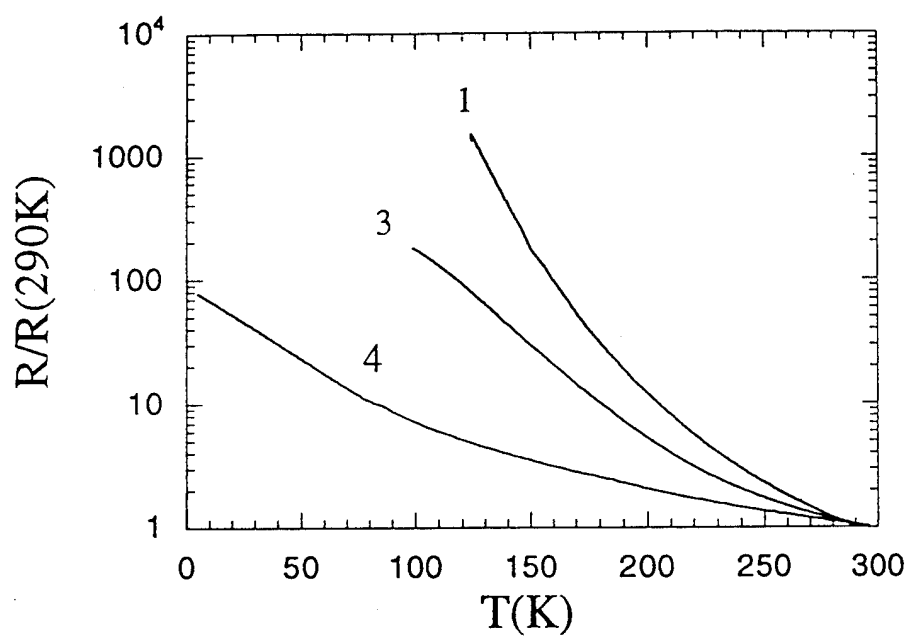
Fig. 6 Normalized temperature-dependent electrical resistivities for different films. Film 4, obtained under 25mTorr of oxygen pressure, has the lowest activation energy.

activation ($\ln\rho \propto 1/T$), variable range hopping ($\ln\rho \propto 1/T^{-1/3}$) or weak-localization ($\rho \propto \ln T$) models [17].

Table 3. Synthesis condition, refined crystal structure and electrical properties of some as-grown films

film	target	P_{O_2} (mTorr)	c-lattice (Å)	Zero Point	Overall B Value	film composition	resistivity (Ω-cm)
1	$Sr_{0.9}CuO_{2-\delta}$	5	3.471	−0.056	3.41	$Sr_{0.48}CuO_{1.48}$	24
2	$Sr_{0.95}CuO_{2-\delta}$	10	3.460	−0.044	3.80	$Sr_{0.63}CuO_{1.63}$	3.2
3*	$Sr_{0.95}CuO_{2-\delta}$	25	3.456	−0.05	3.76	$Sr_{0.75}CuO_{1.75}$	0.04
			3.445		3.56	$Sr_{0.57}CuO_{1.57}$	

* Film 3 consists of two kinds of infinite-layer structures, and the amount of phase 2 ($Sr_{0.68}CuO_{1.68}$) is about 60%.

By analogy to other cuprates based on CuO_2 layers, we expect $SrCuO_2$ to be an electrical insulator. Charge carriers might be injected into the CuO_2 layers by introducing vacancies at Sr sites. Analyses of our films is consistent with such a defect structure, i.e., $Sr_{1-x}CuO_{2-\delta}$. If δ were zero, increasing x should give more charge carriers. As the result, one should observe a decrease in resistivity as x increases. This was not observed in our studies. In the films grown under our conditions, the IL-structure seems to have a tendency to form compositions where most of the Sr vacancies are charge compensated by oxygen vacancies. Therefore, during synthesis at low oxygen pressure, more Sr vacancies are incorporated to compensate for the oxygen deficiency. As a result, there are few free charge carries in the system; thus, the resistivity is very high. Despite the low resistivity and the activation energy, no evidence of superconductivity was observed in film 4 when on cooling to 4.2 K even when a very small current (I=0.01 μA) was used.

Discussion

In the ideal IL structure, all of the atoms are in special positions and the structure can be thought of as alternating Sr^{2+} and CuO_2^{2-} layers. If all atom z positions are either 0.0 or 0.5, the intensities of the (00ℓ) reflections are a measure of the difference in electron density between the CuO_2 layers and the Sr layers. In all of the films made in this study, the intensity ratio (001)/(002) was larger than predicted for the ideal infinite-layer structure. Therefore, only defect mechanisms which cause this ratio to increase are consistent with the experimental data. One defect which could be considered is interstitial oxygen in the Sr layer which would be increase the coordination of copper. This would lead to unreasonably short Cu-O distances of about

1.7Å. Furthermore, adding electron density to the Sr layer is inconsistent with our X-ray analysis of our films.

Another defect model to be considered is intergrowth of Sr_2CuO_3 with $SrCuO_2$ as reported by N. Sugii et al.[10]. Such a model does in fact move the ratio of intensity for the 001 to 002 reflections to larger values. However, this effect is small for this defect. Even for very large concentrations of this defect, agreement with the observed intensity ratios could not be obtained. The fact that this defect requires excess Sr whereas our targets contain excess copper also argues against this defect.

A structural model for our IL layer films consistent with our X-ray analysis is $Sr_{1-x}CuO_2$ (model 2). However, we assume that the high resistivity of our films indicates that the copper oxidation state is very close to two. Therefore, we prefer to the defect formulation $Sr_{1-x}CuO_{1-x}$ (model 1) as a good approximation (Table 4). Another formulation consistent with our X-ray diffraction data for our films is $SrCu_{1+x}O_2$. The interstitial Cu would be in the CuO_2 layers in square planar coordination to oxygen. This would bring the copper oxidation state down, and this might be compensated by Sr vacancies to keep the oxidation state of copper at two, i.e., $Sr_{1-x}Cu_{1+x}O_2$ (model 3).

Table 4. Possible defect models for the infinite-layer structure.

#	Description	Model	(001)/(002) Ratio	c Lattice Constant	Cu Oxidation State
			Defect Concentration Effect On		
1	Charge Compensated Sr and O Vacancies	$Sr_{1-x}CuO_{2-x}$	Increase	Increase	Cu^{2+}
2	Sr Vacancies Only	$Sr_{1-x}CuO_2$	Increase	Increase?	$Cu^{(2+2x)+}$
3	CuO Double Chains[20]	$Sr_{1-x}Cu_{1+x}O_2$	Increase	Increase	Cu^{2+}
4	Intergrowth of Sr_2CuO_3[10]	$Sr_{1+x}Cu_{1-x}O_2$	Increase	Increase	Cu^{2+}
5	Buckling of Oxygen Sheets[18]	$SrCuO_2$	Decrease	Increase	Cu^{2+}
6	Insertion of Apical Oxygen[15]	$SrCuO_{2+x}$	Decrease	Increase	$Cu^{(2+2x)+}$
7	Oxygen Vacancies	$SrCuO_{2-x}$	Decrease	Increase	$Cu^{(2+2x)+}$
8	Sr Shifting off of Ideal Site	$SrCuO_2$	Increase	Increase	Cu^{2+}
9	Cu and O Vacancies	$SrCu_{1-x}O_{2-\delta}$	Increase	Decrease?	$Cu^{(2-2\delta/2-2}$

Given our limited data set, there is no way to differentiate between $Sr_{1-x}Cu_{1+x}O_2$ and $Sr_{1-x}CuO_{1-x}$. In either case, the electrical conductivity rises as x becomes smaller. Thus, the defect most evident from the X-ray diffraction apparently does not produce charge carriers because of a compensating defect If fact, it seems to be easier to produce charge carriers when x is small.

In bulk high-pressure syntheses of IL compounds, both p- and n-doped superconductors have been claimed. However, efforts to prepare p-doped superconducting IL thin films have failed so far[9-12]. One plausible reason may be the difficulty in introducing a sufficient concentration of charge carriers into the CuO_2 sheets. The results of our electrical resistivity measurements, which show increasing conductivity with increasing oxygen pressure, seem to suggest the films are p-doped. Presumably, the films grown under higher oxygen pressures contain more charge carriers. In order to obtain films with the highest possible conductivity, attempts were made to further oxidize the IL structure either by growing films under higher oxygen pressures or by post-annealing of the films in an oxygen atmosphere.

In most cases, non IL phases were obtained when films were grown in higher oxygen pressure ($P_{O_2} > 35$ mTorr), and usually these films were electrical insulators. Occasionally, IL structures with a small amount of unknown phase were obtained. Fresh as-deposited films had very low room temperature electrical resistivities ($\sim 5 m\Omega$-cm). However, these films are very unstable; even at room temperature over night, the IL phase converts to stable insulating phase with a completely different structure(see Fig. 7). S. Sugii et al.[10] observed the intergrowth of Sr_2CuO_3 and $SrCuO_{2-\delta}$ in their IL films. In our case, it is unlikely a transformation of $SrCuO_{2-\delta}$ to Sr_2CuO_3 happens. The lattice parameters of the tetragonal phase Sr_2CuO_3 are: a = 12.648Å; b = 3.9064Å and c = 3.4957Å. We observed a lattice spacing of 6.73Å in the new phase which is longer than d_{200} of Sr_2CuO_3. However, this value is very close to the value of d_{020} of another tetragonal phase, $SrCu_2O_3$.

The as-grown films were also annealed in a furnace at temperatures ranging from 100°C to 300°C. The oxygen pressures used in annealing were 1 atm and 150 atm. In contrast to a previous report[11] that electrical resistivity was reduced by post-annealing of $Sr_{1-x}CuO_{2-\delta}$ in oxygen, we found that the resistivity increased after annealing for all of our films. X-ray diffraction-patterns indicated that IL structures decomposed into other insulating phases after annealing at high temperature (T>200°C), especially for those films initially grown under higher oxygen pressures ($P_{O_2} > 20$ m Torr). There were no obvious differences between the films annealed at 1 atm or 150 atm oxygen pressure. For films grown under lower oxygen pressures, the IL structure remained after annealing at a temperature of 100°C, while the electrical resistivity increased by a few orders of magnitude. Fig. 8 shows the X-ray diffraction patterns of film 2 before and after annealing at a temperature of 100°C for 10 hours. The diffraction intensities were normalized to the (002) peak. Although there are no significant changes in the shapes of the reflections, one can still find differences between the diffraction patterns of the films before and after annealing. First, the (00ℓ) diffraction peak shifts to a lower angle indicating that c-lattice spacing has decreased after annealing in oxygen. Second, the peak intensity ratio of (001)/(002) decreases from about 0.51 to about 0.133. Third, the width of the
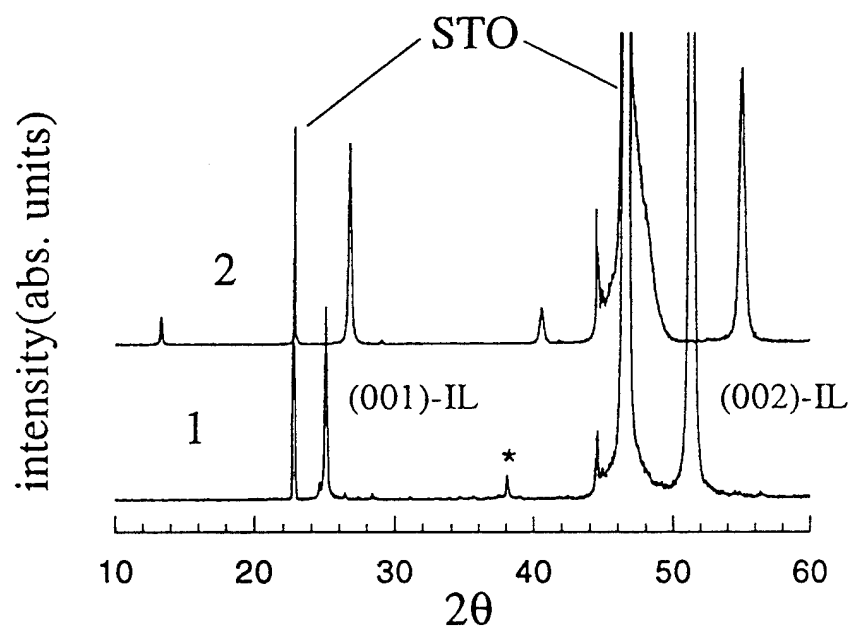
Fig. 7 X-ray diffraction patterns of an IL film grown in 40 mTorr oxygen(1) and after few days at room temperature annealing(2). The marked(*) peak in the fresh film is an unknown phase.
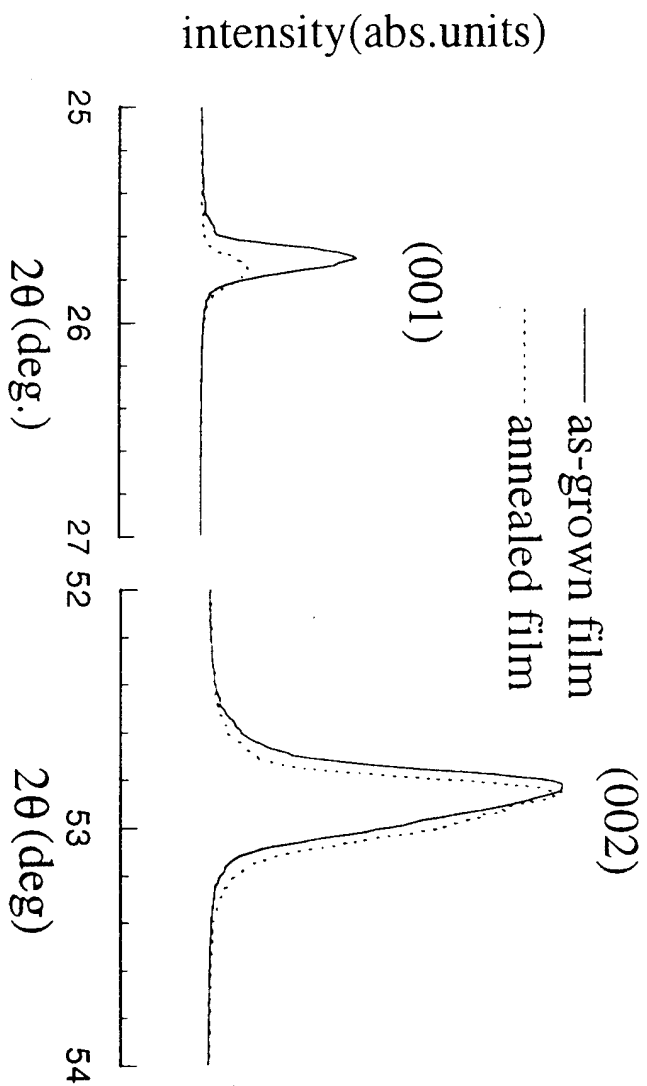
intensity(abs.units)

———— as-grown film

·········· annealed film

(001)

(002)

25　　　　26　　　　27　52　　　　　53　　　　54

2θ (deg.)　　　　　　　2θ (deg)

Fig. 8 X-ray diffraction patterns of film 3 before(solid line) and after 100°C annealing(dashed line) for 10 hours. After annealing, the peak positions shift to lower angles indicating a decrease of the c-axis lattice parameter. The peak intensity ratio of (001)/(002) also decreases from 0.51 to 0.133 after annealing.

In bulk high-pressure syntheses of IL compounds, both p- and n-doped superconductors have been claimed. However, efforts to prepare p-doped superconducting IL thin films have failed so far[9-12]. One plausible reason may be the difficulty in introducing a sufficient concentration of charge carriers into the CuO_2 sheets. The results of our electrical resistivity measurements, which show increasing conductivity with increasing oxygen pressure, seem to suggest the films are p-doped. Presumably, the films grown under higher oxygen pressures contain more charge carriers. In order to obtain films with the highest possible conductivity, attempts were made to further oxidize the IL structure either by growing films under higher oxygen pressures or by post-annealing of the films in an oxygen atmosphere.

In most cases, non IL phases were obtained when films were grown in higher oxygen pressure ($P_{O_2} > 35$ mTorr), and usually these films were electrical insulators. Occasionally, IL structures with a small amount of unknown phase were obtained. Fresh as-deposited films had very low room temperature electrical resistivities (~5mΩ-cm). However, these films are very unstable; even at room temperature over night, the IL phase converts to stable insulating phase with a completely different structure(see Fig. 7). S. Sugii et al.[10] observed the intergrowth of Sr_2CuO_3 and $SrCuO_{2-\delta}$ in their IL films. In our case, it is unlikely a transformation of $SrCuO_{2-\delta}$ to Sr_2CuO_3 happens. The lattice parameters of the tetragonal phase Sr_2CuO_3 are: a = 12.648Å; b = 3.9064Å and c = 3.4957Å. We observed a lattice spacing of 6.73Å in the new phase which is longer than d_{200} of Sr_2CuO_3. However, this value is very close to the value of d_{020} of another tetragonal phase, $SrCu_2O_3$.

The as-grown films were also annealed in a furnace at temperatures ranging from 100°C to 300°C. The oxygen pressures used in annealing were 1 atm and 150 atm. In contrast to a previous report[11] that electrical resistivity was reduced by post-annealing of $Sr_{1-x}CuO_{2-\delta}$ in oxygen, we found that the resistivity increased after annealing for all of our films. X-ray diffraction-patterns indicated that IL structures decomposed into other insulating phases after annealing at high temperature (T>200°C), especially for those films initially grown under higher oxygen pressures ($P_{O_2} > 20$ m Torr). There were no obvious differences between the films annealed at 1 atm or 150 atm oxygen pressure. For films grown under lower oxygen pressures, the IL structure remained after annealing at a temperature of 100°C, while the electrical resistivity increased by a few orders of magnitude. Fig. 8 shows the X-ray diffraction patterns of film 2 before and after annealing at a temperature of 100°C for 10 hours. The diffraction intensities were normalized to the (002) peak. Although there are no significant changes in the shapes of the reflections, one can still find differences between the diffraction patterns of the films before and after annealing. First, the (00ℓ) diffraction peak shifts to a lower angle indicating that c-lattice spacing has decreased after annealing in oxygen. Second, the peak

film	target	PO_2(m Torr)	Model 1 $Sr_{1-x}CuO_{2-x}$	Model 2 $Sr_{1-x}CuO_2$	Model 3 $Sr_{1-x}Cu_{1+x}O_2$
1	$Sr_{0.9}CuO_{2-\delta}$	5	x=0.41	x=0.36	x=0.24
2	$Sr_{0.95}CuO_{2-\delta}$	10	x=0.27	x=0.23	x=0.16
3*	$Sr_{0.95}CuO_{2-\delta}$	25	x=0.16	x=0.14	x=0.09
			x=0.32	x=0.28	x=0.19

* Film 3 consists of two kinds of infinite-layer structures, and the amount of phase 2 ($Sr_{0.68}CuO_{1.68}$) is about 60%.

intensity ratio of (001)/(002) decreases from about 0.51 to about 0.133. Third, the width of the rocking curve of (002) peak decreases about 20% indicating an improvement of crystallinity. The changes are irreversible by reannealing the films in oxygen vacuum. The first two observations are consistent with a decrease in the concentration of defects in the structure. Calculations based on the observed peak intensities indicate the stoichiometry of the film after annealing is $Sr_{0.84}CuO_{1.84}$.

In our preferred model, there are vacancies at both the Sr and O sites for as-grown samples sucs as film 2. During the oxygen annealing, as oxygen atoms diffuse into the film, Sr vacancies might also be filled due to the charge-balance considerations. This picture is consistent with the results of decreasing of c-lattice parameter and increasing resistivity after annealing. For this explanation to be plausible, there must be a source of Sr. Considering the fact that the Sr content of the target is larger than that of film 2, one may argue that there is a small amount of a Sr-rich phase coexisting with the IL phase. If such a Sr-rich phase exists, it must be poorly crystalline and/or non-epitaxial to explain why it does not show up in the diffraction patterns of the as-grown films.

Conclusions

A series of metastable IL $Sr_{1-x}CuO_{2-\delta}$ thin films were deposited under various oxygen pressures. The structural and electrical properties of the films are very sensitive to the oxygen pressure. The highest defect concentrations and highest electrical resistivities were found in the films prepared at the lowest oxygen pressure. The electrical conductivity as well as structural instability increased for samples prepared at higher oxygen pressure. Table 5. Defect concentration of films as calculated for defect models 1,2 and 3.

References

1. T. Siegrist, S. M. Zahurak, D. W. Murphy and R. S. Roth, *Nature(London)* **334**, 231(1988).
2. M. G. Smith, A. Manthiram, J. Zhou, J. B. Goodenough and J. T. Markert, *Nature(London)* **351**, 549(1991).
3. G. Er, Y. Miyamoto, F. Kanamaru, M. Takano, Y. Bando and Y. Takeda, *Physica C*, **181**, 206(1991).
4. N. Ikeda, Z. Hiroi, M. Azuma, M. Takano, Y. Bando and Y. Takeda, *Physica C*, **210**, 367(1993).
5. N. Azuma, Z. Hiroi, M. Takano, Y. Bando and Y. Takeda, *Nature(London)* **356**, 775(1992).
6. M. Takano, M. Azuma, Z. Hiroi and Y. Bando, *Physica C*, **176**, 441(1991).
7. Z. Hiroi, M. Takano, M. Azuma and Y. Takeda, *Nature(London)* **364**, 315(1993); Z. Hiroi, M. Azuma and M. Takano, *Physica C*, **208**, 286(1993).
8. S. Adachi, H. Yamauchi and N. Mori, *ISTEC Journal*, **7**, 21(1994).
9. D. D. Norton, B. C. Chakoumakos, E. C. Jones, D. K. Christen and D. H. Lowndes, *Physica C*, **217**, 146(1993).
10. N. Suggi, M. Ichikana, K. Hayashi, K. Kubo and K. Yamamoto, *Physica C*, **213**, 345(1993).
11. R. Feenstra et al. *Physica C*, **224**, 300(1994).
12. H. Yakabe, A. Kume, J. Wen, M. Kosuge, Y. Shiohara and N. Koshizuka, *Physica C*, **232**, 371(1994).
13. H.P. Klug and L.E. Alexander, *X-Ray Diffraction Procedures* (Wiley & Sons Inc., New York, 1954).
14. C.G. Darwin, *Phil. Mag.*, [6], **43**, 800 (1922).
15. Jinhua Ye and K. Nakamura, *Phys. Rev.*, **B50**, 7099(1994); *Phys. Rev.*, **B48**, 7554(1993).
16. J. L. MacManus-Driscoll, J. A. Alonso, P. C. Wang, T. H. Geballe and J. C. Bravman, *Physica C*, **332**,
17. Koh-ichi Kubo and H. Yamauchi, *Phys. Rev.*, **B49**, 1289(1994).